

# Performance of a single loop thermoacoustic engine model installed with two conical segments at heat exchangers end

Nurpatricia<sup>1,\*</sup>, Agus Dwi Catur<sup>2</sup>

<sup>1,2</sup>Mechanical Engineering Dept., Faculty of Engineering, Mataram University, INDONESIA

\*Corresponding Author: nurpatricia@unram.ac.id

**ABSTRACT:** A single-loop thermoacoustic engine model has been built with Delta-EC simulation. This engine model has capability in utilizing heat source from flue gas of low-grade biomass combustion. A promising feature of this model is for low cost implementation due to abundant availability of low-grade biomass in the form of agricultural waste at rural area. This engine model is inserted with two conical segments in two location to represent actual minor losses that occurred at that locations. Simulation was conducted through Delta EC software in order to examine the model performance at various heat input amount to represent actual operational conditions. On a certain setting of the model parameters, the results show that the engine capable to operate at a range of 440 watts. The highest heat input amount suggested to be limited to 815 watts due to real condition operational. The lowest realistic heat input amount is 375 watts due to restriction on energy flow balance through engines segments involved.

## NOMENCLATURE

Symbol	Description	Unit
$A$	Area	$m^2$
$E$	Acoustic energy	watt
$f$	Complex factor	
$g$	Complex factor	
$Im$	Imaginary part of complex variable	
$K$	Minor losses coefficient	
$p$	Pressure	$Pa$
$Q$	Heat	watt
$Re$	Real part of complex variable	
$T$	Temperature	$K$
$U$	Volumetric flow rate	$m^3/s$
$u$	Velocity	$m/s$
$W$	Length	$m$
$x$	x-axis, x-direction	

## Greek letter

$\theta$	Phase	$deg$
$\eta$	Efficiency	%

## Subscripts

H	heat
A	acoustic
m	mean
1 to 6	position in x-direction

Date of Submission: 24-11-2023

Date of acceptance: 06-12-2023

## I. INTRODUCTION

In the last few decades, thermoacoustic engine technology has emerged. This engine is a type of external combustion engine without essential moving parts. The engine consists of several main components which all placed in the main channel which forms an engine loop. It capable of utilizing heat sources from various kinds, including the heat from untreated biomass combustion that categorized as low-grade energy source. The heat energy from low grade energy source is then converted into acoustic energy in a thermoacoustic engine component of a porous material known as regenerator. Acoustic energy generated by the thermoacoustic engine can be further converted into mechanical energy, in the way of extracting the pressure amplitude from the acoustic waves [1].

The ability of this type of engine be able to utilize untreated biomass as it heats source opens a promising possibility of contribution to global climate change mitigation. The global climate change is one of the current challenges for humanity, so awareness has emerged to begin diminishing the utilization of fossil fuels which are still the main supply for global energy fulfillment, reaching 81% according to the World Bioenergy Association [2]. The use of these fossil fuels is considered to be the largest contributor to greenhouse gas emissions, which are the main driver of climate change. Because of this, the use of fossil fuels has begun to be replaced by renewable energy source such as biomass. Apart from being a household fuel, biomass can also be used as a fuel for internal combustion engines and external combustion engines. Moreover, biomass needs to be purified first to become a high-grade fuel type so that it can be used in internal combustion engines. Availability of technology needed for processing biomass to become high grade fuel type for small scale, for example for household needs in rural areas, is still limited. This limitation is mainly due to the needs of supporting equipment in the process which is still quite complex, and initial installation costs still relatively expensive [2]. These two factors are among restrictions the use of biomass fuel for internal combustion engines. Therefore, biomass as a fuel is more common introduced in the field of external combustion engine applications.

The engine was built by Yazaki et al [3] is one of successful setups for single looped thermoacoustic engine. In this arrangement, engine utilizes traveling-wave type of sound waves, which is propagates through entire loop channel. Three main components of the engine are hot heat exchanger, cold heat exchanger, and regenerator, which are placed in the loop. Thermoacoustic core, that is regenerator, was observed as one of important parameter that roles the ability of the model to generates acoustic power. The characteristic transverse length of sandwiches solid layer in the regenerator has quadratic effect on the minimum onset temperature ratio, the minimum temperature ratio applied so that a spontaneous acoustic wave oscillates. The engine, which is sets in travelling-wave engine arrangement mode, was successfully generate about 200 W/m<sup>2</sup> acoustic power. It amplifies acoustic power with gain 1.2, which is means net power of about 20% than those of input acoustic intensity incoming from cold end side of regenerator [3]. High axial average velocity causes large viscous losses which in turn significantly reduce the engine efficiency. Backhaust and Swift [4] construct for the first time a torus and resonator type of thermoacoustic Stirling engine, which is known as TASHE (Thermoacoustic Stirling Heat Engine), almost one year after Yazaki et al [2] published their one wavelength looped engine. The Backhaust and Swift's engine is considered as a variant that developed from a single loop engine arrangement, although both of them developed separately. Dimensions and performances of TASHE can be found in Backhaust and Swift [4]. The looped tube of the engine is filled with Helium and it works at a frequency of 80 Hz. The engine's efficiency achieved 30%, corresponds to 42% theoretical maximum Carnot efficiency, is higher than other pistonless thermal engine. Apart from the inner working fluid setting parameters, the main construction difference of the two type of engine arrangement is the introduction of resonator branch in the TASHE engine.

Nurpatria et al [5] construct a thermoacoustic engine model, which is capable in utilizing flue gas from biomass combustion as a heat source. This model has parameters that derived from advantageous key factors of Yazaki et al [3] and Backhaust and Swift [4] engine designs. This engine model designed with special feature in hot heat exchanger arrangement which allows it to receive heat from direct flue gas flow of low-grade biomass combustion. Small scale implementation of the engine is promising mostly in rural area, considering that abundant availability of low-grade biomass such as agricultural waste in that area. The loop of this engine is modeled as continuous channel without any bends or channel area change. As the consequences, the working fluid inside the loop is flow without experiencing any type of energy loss. This idealization behavior is unmatched with the fact that the actual flow undergoes energy loss due to surface friction or pressure drop. Nurpatria and Catur [6] further develop the previous model of Nurpatria et al [5] with additional of minor losses sub model of two conical segments. The main objective of this paper is to present simulation performance result of Nurpatria and Catur [6] model, after two conical segments addition.

## **II. SIMULATION SETUP**

### **A. Engine Modelling**

The thermoacoustic engine model presented in this article is shown in Figure 1. The simulation method used to determine the model performances is through one-dimensional Delta EC simulation, conducted in Version 6.2 package of Ward et al [7]. Through this open source Delta EC software, the engine body divides into several individual segments. Initial simulation position correlated to  $x = 0$  in the engine's loop is at cross section 2, or marked as point 2 at Figure 1. Acoustic energy is generated in the regenerator (REG), segment 3-4, of the engine. The regenerator material is modeled to be composed from porous material with such a small pore size equivalent to the thickness of thermal penetration depth. The machine loop starts from point 5 to point 2. In this loop, acoustic energy  $E$  that flows, varies depending on its precise location in the loop. If the flow losses do not occur, the acoustic energy in the narrow gap at straight channel segment between point 2 and an earlier

closest point, for example point 1, also does not change. The same condition also applicable in the short straight pipe segment from point 5 to 6, which is in the x-direction flow.

Hot flue gas biomass combustion is modeled as a source converted acoustic energy generated by regenerator. The heat energy is required to create a working fluid temperature gradient between two end cross section of the regenerator, from point 3 to 4 in figure 1. The working fluid temperature gradient along the regenerator is made possible by the difference in the amount of heat supply in the cold heat exchanger (CHX) and hot heat exchanger (HHX). In Figure 1, CHX located at segment 2-3, and HHX is at segment 4-5. The  $E_4$  acoustic energy amplified by REG that comes out of the HHX flows in the x direction in the loop and becomes  $E_3$  feed energy which goes back into CHX, which is re-amplified by REG. A potential acoustic energy loss in the engine's working fluid flow, in terms of decreasing acoustic energy, possibly occur at the interface of two segments with different cross-sectional area. In the case of engine model in Figure 1, if the cross-sectional area of loop  $A_1$  or  $A_6$  are the same as the cross-sectional areas of CHX and HHX, that are  $A_2$  and  $A_5$ , then there will be no loss of flow at these two locations.

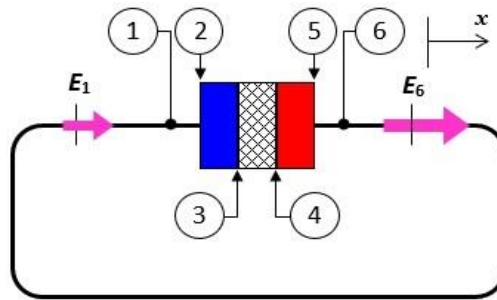


Fig. 1 The single looped thermoacoustic engine model

Acoustic energy that flows throughout all thermoacoustic engine segments which is  $E$  in Equation 1, induced by two acoustic wave components, (a) the traveling wave pressure wave  $p$  and (b) the volumetric flow rate  $U$ . As an exception, acoustic energy generation in the regenerator's pore follows Equation 2, where  $p$  and  $U$  are also involved. The variables  $E$ ,  $p$  and  $U$  are in complex domain. Therefore, differences in  $p$  and  $U$  oscillations lead to a specific phase at each different location along the engine's body. So that the phase difference also has an effect on the acoustic energy difference in two cone segments placed at two different locations in the engine's loop.

The acoustic energy flowing through a certain segment in the engine model, including the loop segment, is according the equation from Swift [8]. The pressure difference between the two ends of a segment is  $\Delta p$ , the volume flow rate in the segment is  $U$ , and  $\theta$  is the phase angle difference of each  $p$  and  $U$  oscillation. The acoustic energy flowing in a straight channel segment, for example between points 1 and 2 in Figure 1, is calculated based on the difference pressure between both endpoints of the segments. Equation 1 applies to all segments, except for the regenerator.

$$E = \frac{1}{2} |\Delta p| |U| \cos(\theta) \tag{1}$$

Acoustic energy generated from regenerator segment can be calculated with Equation 2 [8]. Statement in this equation is in the complex domain, so that the pressure oscillation  $p$  and the volume flow rate  $U$  are also in the complex domain. Moreover, acoustic propagation is then represented by the statement of real component,  $Re[]$  in terms on the left side and imaginary component  $Im[]$  in the second right side of it.

$$\frac{1}{2} Re[gpU] = \frac{1}{2} \frac{1}{T_m} \frac{dT_m}{dx} Re[pU] Re[f_\kappa] + \frac{1}{2} \frac{1}{T_m} \frac{dT_m}{dx} Im[pU] Im[-f_\kappa] \tag{2}$$

Positive temperature gradient,  $(dT_m/dx)$ , that is introduced to the regenerator is gained from the difference between heat rate input  $Q$  at CHX and at HHX. If the CHX is maintain at the ambient temperature, or at the engine's mean temperature  $T_m$ , the heat input of the engine is simply affected by heat injected into the HHX,  $Q_H$ . Thus, the overall engine efficiency is known from equation 3 [4,8].

$$\eta_{H-A} = (E/Q_H) \tag{3}$$

Acoustic energy always attenuated along positive  $x$  direction. The only location acoustic energy is generated is inside regenerator, at its porous filling material. So that the acoustic energy generated by engine  $E$

is the amplification of acoustic energy feed that exits from CHX which is equals to that incoming to the regenerator, point 3 in figure 1, into acoustic energy that exits the regenerator at point 4. The overall efficiency is simply the ratio between the two, E and Q<sub>H</sub>.

**B. Minor Losses**

Cross section area, or corresponds to diameter, at some certain locations of the loop channel in Figure 1 usually changes. It accommodates the difference in optimum diameter of each segment that obtained from simulation procedures. The engine model of Nurpatra et al [5] is built with some simplifications, including that the loop channel composed without bends, diameter alteration, or conical segments. Such idealization assumption lead to impracticality in the manufacturing process. The real engine loop channel usually assembled from several single piece of pipes and bends that connected together to form a complete single loop. As a consequence, the engine model must be redefined to accommodate those various different physical geometries form of the channel. That more realistic channel model in turn lead to the needs of modelling the flow losses that occurred at those geometries. Flow losses in bends and diameter changes are commonly termed as minor losses, which is added in Nurpatra and Catur [6]. Two minor losses that occurred at those segments are placed before CHX at 1-2, and after HHX at 5-6.

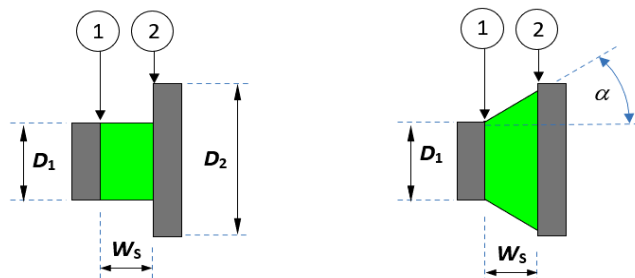


**Fig. 2 Geometry of (a) straight segment, compared to (b) cone segment**

Minor losses ( $\Delta p$ ) in the loop of a thermoacoustic engine is adapted from Ward et al [7]. It depends on coefficient K, and the flow velocity u, in equation 4. The velocity u is volumetric flow rate in the complex expression U from equation 1 or 2, which flows in reciprocal manner regarding to the x direction. As a consequence, numeric value of K factor in equation 4 should be set differently for either positive x-direction flow (K+) or negative x-direction flow (K-). Pressure p in x direction will decrease due to inner friction of working fluid particles flowing through inner wall surface roughness, and it indicates by minus sign in (4). In conducting the simulation, both K+ and K- is set simultaneously inside the software through sub model for each conical segment [6].

$$\Delta p = -\frac{1}{2}Ku^2 \tag{4}$$

This paper presenting performance of the engine model at various heat input so that the effect of two cone segments causing minor losses be able to be revealed.

**Table(1). Cone segment geometrical parameters**

Segment		Parameter			Setting
		Name	Symbol	Unit	
1	Cone 1	Length	W <sub>s1</sub>	mm	12
		Area 1 In	A <sub>1</sub>	cm <sup>2</sup>	90
		Area 2 Out	A <sub>2</sub>	cm <sup>2</sup>	100
2	Cone 2	Length	W <sub>s2</sub>	mm	12
		Area 5 In	A <sub>5</sub>	cm <sup>2</sup>	90
		Area 6 Out	A <sub>6</sub>	cm <sup>2</sup>	100

It is shown in figure 2, a straight segment figure 2(a) compared to a cone segment in figure 2(b). The first cone segment inserted into the model is placed at cross section 1 to 2, and the second one is at 5 to 6 (not shown in figure 2) but in reverse convergent direction. The cone diameter, or hydraulic diameter, of the first cone is gradually enlarges from its smallest inner diameter D<sub>1</sub> at 1 to become largest inner diameter D<sub>2</sub> at 2. So that the minor losses coefficient applied to the model in Figure 1 become K+ sets at location 1, and K- sets at location 2. In the case of the second cone, K+ sets at 5, and K- sets at 6, Figure 1 [6,8]. This two K value at different setting correlated to two different type of obstruction minor losses, gradual cross section enlargement losses and gradual cross section contraction losses.

Table 1 shows geometrical parameter of both cone segment of the thermoacoustic engine presented in this paper. Previous engine model loop length, that is length from point 5 to 2 in figure 1, is 174 cm [6]. The engine loop length of current engine model presented in this paper is also kept at the same loop length. Cone 1 length  $W_{s1}$  replaces the same length from 1 to 2 at the straight model. Also, cone 2 length  $W_{s2}$  is replaces straight length from 5 to 6.

### III. RESULTS AND DISCUSSION

The model that inserted with two cone segments shows a typical acoustic energy (E) level along its loop as shown in Figure 3. This model is the first obtained convergent model from the result of previous simulation, Nurpatra and Catur [6]. Acoustic energy level of this model is varying along the loop corresponds to a certain x position. The point  $x = 0$  is set before CHX, that is before point 1 in Figure 1. Acoustic energy enters CHX is 159 watts, at  $x = 0,20$  m as shown in figure 3.

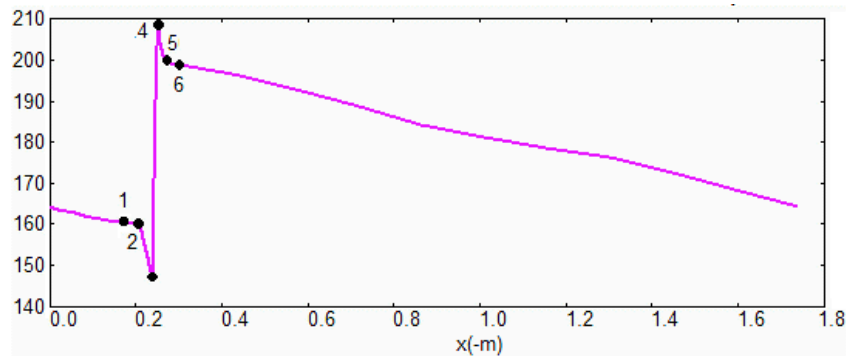


Fig. 3 Acoustic energy inside the engine inserted with two cone segment model

The engine model of Nurpatra and Catur [6], is the most promising dimension if this model intended to be constructed. This paper presented some insight of its performance in receiving various amount of heat input, to mimic the real operational conditions. Acoustic energy from the regenerator is increase as indicated from point 3 to point 4 in figure 3. The source of this acoustic energy is come from supplied heat that is injected into the HHX, which is in turn acts as the hot end of temperature, or  $T_h$  in table 2. Temperature gradient is then maintained to be exist throughout the conversion process, that is the difference between  $T_h$  and  $T_c$  from table 2. Figure 3 shows the highest acoustic energy generated by the engine is at point 4, that is  $E_4 = 204.1$  watt. Acoustic energy along the loop is constantly attenuated, shown by curve declination from hot exit of HHX at point 5 to cold inlet of CHX at point 2. Step energy loss occurred at both heat exchanger, at CHX from point 2 to 3, and at HHX from point 4 to 5. The slope attenuation at the whole channel loop segment is addressed as an effect of inner channel wall friction loss [9]. On the other hand, in the case of both heat exchanger, the steep slope energy attenuation is affected by additional loss in inner pipe bundle [9].

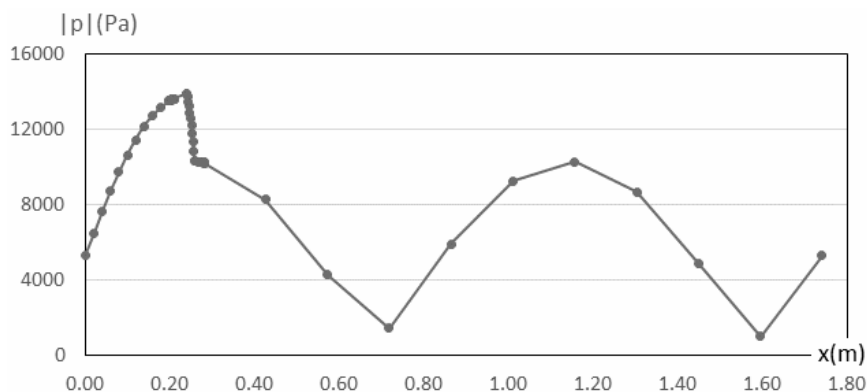


Fig. 4 Pressure wave inside the engine

Figure 4 shows typical pressure along the engine's loop. First to note that the acoustic energy generation in regenerator, marked as point 3 to 4 in figure 3, correlated to the steep pressure drop shown in figure 4. This amount of pressure energy is converted into acoustic energy along with velocity energy that in the correlation of equation 1. Second thing to note is on the placement of regenerator. It is sets in the position where pressure in its highest magnitude, at  $x = 0,22$  m.

Based on above mention Nurpatria and Catur [6] model, the model with  $Q_{in} = 815$  watt in table 2, is undergoes a further simulation in order to investigated its performance on a various of heat input amount. Result of that simulation is also in the table 2. With 815 watts heat input, surface hot temperature of each pipe outer diameter in the pipe bundle of HHX reach 723 K, or 450°C. Increasing the heat input, such as 915 watts, lead to two different issue that are decreasing in heat to acoustic efficiency from 7.0% into 6.2%, and pipe surface temperature exceeds 450°C. The first one is clearly undesired, while the second become an operational restriction due to cracking issue at pipe material welding joint at 450°C or above [1,4].

**Table(2). Engine model performance at various heat input**

HHX		CHX		Delta EC Model Performance			
$Q_{in}$	$T_h$	$Q_{out}$	$T_c$	$\Delta Q$	$\Delta T$	$E_{dot}$	$\eta_{H-A}$
(watt)	(K)	(watt)	(K)	(watt)	(K)	(watt)	(%)
215	684	318	300	-103	384	57	26.6
315	691	318	300	-3	391	57	18.1
<b>375</b>	<b>695</b>	<b>318</b>	<b>300</b>	<b>57</b>	<b>395</b>	<b>57</b>	<b>15.3</b>
415	697	318	300	97	397	57	13.8
515	704	318	300	197	404	57	11.1
615	710	318	300	297	410	57	9.3
715	716	318	300	397	416	57	8.0
<b>815</b>	<b>723</b>	<b>318</b>	<b>300</b>	<b>497</b>	<b>423</b>	<b>57</b>	<b>7.0</b>
915	729	318	300	597	429	57	6.2

Decreasing the heat input, from 815 watts to 215 watts in this case, shows some characteristics of this model. Surface cold temperature of each pipe outer diameter in the pipe bundle of CHX forced to be constant at 300 K or 27°C, considering the ambient cooling fluid used is exposed to atmospheric air. So that heat rejected  $Q_{out}$  from CHX is also constant at 318 watts. Acoustic energy ( $E_{dot}$ ) generated by regenerator at various heat input is also constant at 57 watts. This model is shows a less sensitive output to adapt with changing heat input, and this is a bias characteristic compared to actual behavior of a known real engine ever built [3,4]. Moreover, the model shows a proper simulation result up to heat input as low as 375 watts, considering the minimal amount of injected heat into hot heat exchanger should be converted into sum of both acoustic energy generated inside regenerator and heat rejected from cols heat exchanger. So that the simulation result obtained with heat input lower than 375 watts considered as unrealistic behavior of this model.

#### IV. CONCLUSION

The engine model is capable to convert heat energy into acoustic energy at various heat input to mimic the actual operational condition. The realistic performance result of the model is restricted between 375 watts and 815 watts. Heat input lower limit is due to the fact applied for input and output energy balance among engine components involved. Heat input upper limit sets considering the fact of physical material properties in deal with high temperature. Model sensitivity in responds to alteration of heat input needs some improvement.

#### REFERENCES

- [1]. Elferink M, Steiner T. [2019] “Thermoacoustic waste heat recovery engine - Comparison of simulation and experiment” Proceedings of Meetings on Acoustics, Vol. 35, No. 065002
- [2]. Sertolli A., Gabnai Z., Lengyel P., Bai A. [2022] “Biomass potential and utilization in worldwide research trends - A bibliometric analysis” Sustainability, Vol. 14, No. 5515
- [3]. Yazaki T., Iwata A., Maekawa T., Tominaga A. [1998] “Traveling wave thermoacoustic engine in a looped tube” Physical Review Letters, Vol. 81, No. 15
- [4]. Backhaus S., Swift G.W. [2000] “A thermoacoustic Stirling heat engine - Detailed study” Journal Acoustic Society of America, Vol. 107, No. 6
- [5]. Nurpatria, Susana I G.B., Joniarta I W., Nurchayati, Tira H.S. [2021] “Peningkatan efisiensi konversi energi mesin termoakustik” Prosiding SAINTEK LPPM Universitas Mataram, Vol. 3, pp.369-373
- [6]. Nurpatria, Catur A. D. [2023] “Minor Losses Of Cone Segments Insertion Into Single Loop Thermoacoustic Engine Model” IJPSAT, Vol.39 No.1, pp.177-183
- [7]. Ward B., Clark J., Swift G. [2008] Design Environment for Low-amplitude Thermoacoustic Energy Conversion (Delta EC) - Version 6.2 Users Guide, Los Alamos National Laboratory
- [8]. Swift G [2001] Thermoacoustics - A unifying perspective for some engines and refrigerators, Condensed Matter and Thermal Physics Group - Los Alamos National Laboratory, 5th Draft
- [9]. Yiyi M., Xiujuan X., Shaoqi Y., Qing L. [2015] “Study on minor losses around the thermoacoustic parallel stack in the oscillatory flow conditions” Physics Procedia, No. 67, pp.485-490